Article

Immunomodulatory Effects of *Atractylodes lancea* in Healthy Volunteers with Dosage Prediction for Cholangiocarcinoma Therapy: A Modelling Approach

Teerachat Saeheng [1,2], Juntra Karbwang [3] and Kesara Na-bangchang [1,2,3,*]

[1] Center of Excellence in Pharmacology and Molecular Biology of Malaria and Cholangiocarcinoma, Chulabhorn International College of Medicine, Thammasat University (Rangsit Campus), Pathumthani 12120, Thailand

[2] Graduate Program in Bioclinical Science, Chulabhorn International College of Medicine, Thammasat University (Rangsit Campus), Pathumthani 12120, Thailand

[3] Drug Discovery and Development Center, Office of Advanced Science and Technology, Thammasat University (Rangsit Campus), Pathumthani 12120, Thailand

[*] Correspondence: kesaratmu@yahoo.com or nkesara@tu.ac.th; Tel.: +66-2564-4440-1800

Abstract: Background and Aims: According to a recent study on the immunomodulatory activity of Atractylodes Lancea (Thunb.) DC. (AL) in healthy Thai subjects, AL significantly inhibited the production of key pro-inflammatory cytokines while stimulating the production of immune cells. However, no maximum tolerated dose (MTD) and phase 2A dosage regimens were reported. The study aimed to evaluate the immunomodulatory effects of *Atractylodes lancea* (Thunb.) DC. (AL) in healthy subjects, and to recommend optimal dose regimens for intrahepatic cholangiocarcinoma (iCCA) based on toxicity criteria. **Methods:** A physiologically based pharmacokinetic (PBPK) model, combined with the toxicological approach and the immunomodulatory effect, was used for dose-finding. The safety and efficacy of each AL regimen were evaluated based on the previous study. At least a once-daily dose of 1000 mg AL significantly suppressed the production of all pro-inflammatory cytokines while significantly increasing the number of peripheral immune cells. **Results:** The developed PBPK model predicted the clinically observed data well. No significant differences in SII index values were found, but a difference in the lymphocyte-monocyte ratio was found on day 4. The dosage regimen for phase 2A is a once-daily dose of 1500 or 2000 mg. Preliminary results in phase 2A revealed that a once-daily dose of 2000 mg had a significantly higher median overall survival, progression-free survival, disease control rate, and inhibition of increased tumor size without toxicities compared with control. **Conclusions:** A PBPK model, in conjunction with a toxicological approach, could assist in finding the potential dosage regimens for a clinical study, including herbal medicine.

Keywords: pharmacokinetics; atractylodin; immunomodulatory; physiologically based pharmacokinetic model; PBPK; pharmacokinetic modeling

1. Introduction

Heterogeneous recruitment of various immune cells, i.e., CD8+, CD4+, natural killer (NK) cells, tumor-associated macrophages (TAMs), cancer-associated fibroblasts (CAFs), and myeloid-derived suppressor cells (MDSCs) constitute an integral part of the tumor

microenvironment (TME) of cholangiocarcinoma (CCA) [1]. With increasing knowledge of the TME, intrahepatic cholangiocarcinoma (iCCA) has been classified into four unique subtypes: immunological desert, immunogenic, myeloid, and mesenchymal [2]. This classification offers a new paradigm for iCCA therapy. Immune checkpoint inhibitors (ICIs) such as nivolumab and pembrolizumab are currently the research focus of iCCA therapy. PD1 and PD-L1 are programmed cell death proteins expressed in immune and cancer cells, respectively [3]. Anti-PD1 and anti-PD-L1 antibodies have been shown to improve the therapeutic efficacy in advanced-stage CCA patients with or without metastases [3]. In addition, nivolumab has been reported to enhance the clinical effectiveness of the first-line treatment gemcitabine/cisplatin when combined in treatment-naive patients with advanced CCA [4]. Immunomodulators that regulate the TME thus present a novel treatment strategy for patients with advanced-stage CCA.

Atractylodes lancea (Thunb) DC. (AL) is widely distributed in East Asia and has been extensively employed in traditional Chinese medicine (TCM) to treat various ailments, including influenza and digestive issues, primarily in China. This organism is categorized as a member of the Asteraceae family, sometimes called Compositae, within the plant kingdom. AL is composed of sesquiterpenoids, monoterpenes, polyacetylenes, phenolic acids, and steroids, including atractylodin (14%), β-eudesmol (6%), atractylon (2%), and hinesol (1%).

A recent study on the immunomodulatory activity of AL in healthy Thai subjects (atractylodin as the active ingredient) revealed that a once-daily dose of 1000 mg AL administered for 21 days significantly inhibited the production of key pro-inflammatory cytokines while stimulating the production of immune cells [5]. Due to its potential immunomodulatory activity, AL could be a viable therapy for iCCA. A safe first-in-human (FIH) dose of AL has been proposed based on the maximum recommended starting dose (MRSD) determined in animal models [6]. There is, however, no reported maximum tolerated dose (MTD) and suggested dosage regimens for a phase 2A clinical study in the literature [5].

Physiologically based pharmacokinetic (PBPK) modeling is a technique accepted by the US FDA and EMA for drug submission that predicts optimal dose regimens for various disease therapies, including cancer therapeutics [7,8]. This approach avoids recruiting unnecessarily large numbers of research participants for clinical trials. This approach might be particularly advantageous for determining the optimal dose regimens of candidate drugs, notably anti-cancer drugs. The present study aimed to evaluate the immunomodulatory effects of AL in healthy subjects based on information from previous research [5,6] to predict FIH, MTD, and phase-2A dosing regimens of AL.

2. Results

2.1. Pharmacokinetics Analysis

The AUC_{0-inf}, C_{max}, V_z/F, CL/F, and $t_{1/2}$ for group 1 (day 1) and group 2 (days 1 and 21) are summarized in Table 1.

Table 1. Pharmacokinetic parameters following a single dose of 1000 mg of AL administered (group 1), and daily doses of 1000 mg of AL (group 2) administered for 21 days.

Number	Parameter	Value
	Group 1 (Day 1)	
1	AUC (μmol·h/L)	0.55
2	C_{max} (μmol/L)	0.25
3	V_z/F (L/kg)	11.33
4	CL/F (L/h/kg)	5.01

5	$T_{1/2}$ (h)	1.63
Group 2 (Day 1)		
6	AUC (µmol·h/L)	0.64
7	C_{max} (µmol/L)	0.28
8	V_z/F (L/kg)	14.12
9	CL/F (L/h/kg)	7.55
10	$T_{1/2}$ (h)	1.27
Group 2 (Day 21)		
11	AUC (µmol·h/L)	0.72
12	C_{max} (µmol/L)	0.30
13	V_z/F (L/kg)	13.41
14	CL/F (L/h/kg)	8.04
15	$T_{1/2}$ (h)	1.14

AUC: area under the plasma concentration–time curve; C_{max}: maximum plasma concentration; V_z/F: volume of distribution; CL/F: apparent clearance; $T_{1/2}$: terminal half-life.

2.2. Immunomodulatory Effect of AL (Atractylodin): Effects on Circulating Peripheral Blood Cells, Immune Cells, and Pro-Inflammatory Cytokines

AL as an OD dose of 1000 mg administered for 21 days markedly decreased the production of the pro-inflammatory cytokines IL-17A, IFN-γ, TNF-α, IL-10, IL-6, IL-4, and IL-2 (Table S2). On the other hand, no significant decrease in the levels of these cytokines was observed in the placebo group (Table S2). In addition, AL significantly decreased the number of total lymphocytes and CD4+ cells (Table S3) while increasing B cells, T cells, CD8+ cells, NK cells, and the CD4+/CD8+ ratio (Table S3). In the placebo group, T cells, CD4+ cells, CD8+ cells, B cells, and NK cells were significantly reduced (Table S3). There was a significant change in LMR on day 4 in the AL-treated group and on day 22 in the placebo group (Table S3). The SII index values were comparable between the two groups (Table S3). The mean (±SD) of cytokine levels, immune cells, SII-index, and peripheral blood ratio on each day are shown in Figures 1–4.
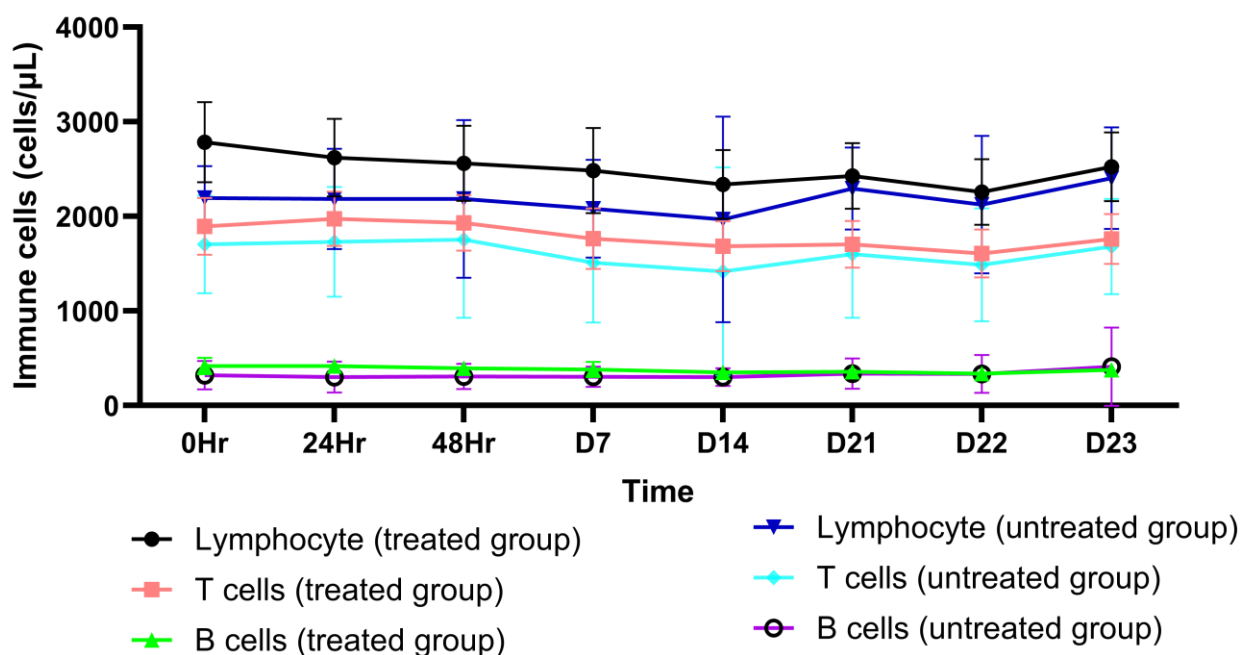

Figure 1. A comparison of different interleukin (IL) levels between the treated group and the untreated group for each day.
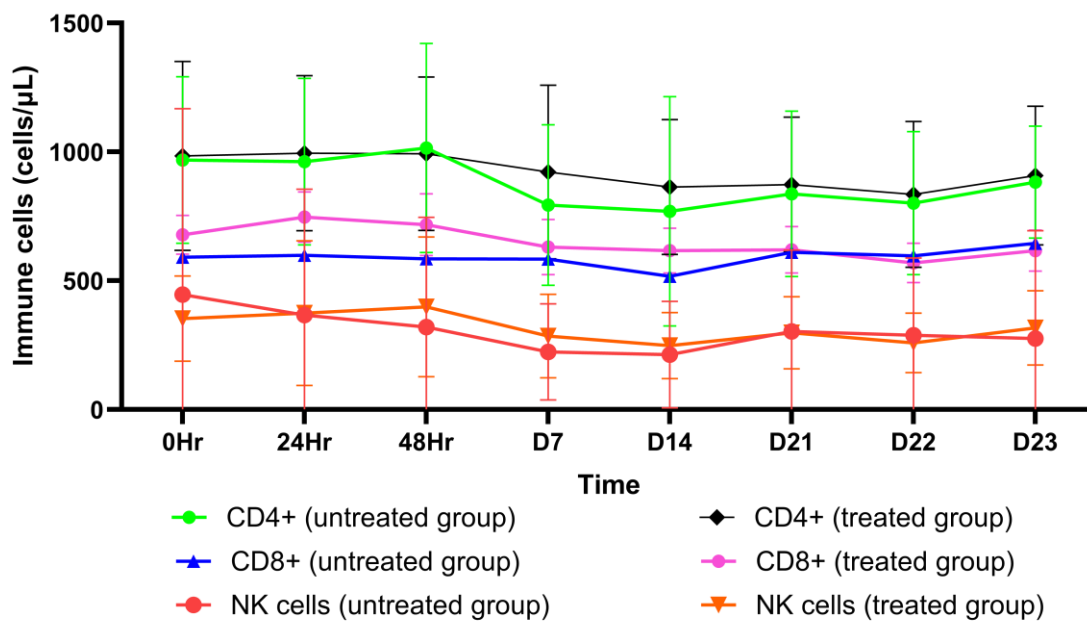
Figure 2. A comparison of different interleukin (IL) levels between the treated group and the untreated group for each day. NK cells: natural killer cells.
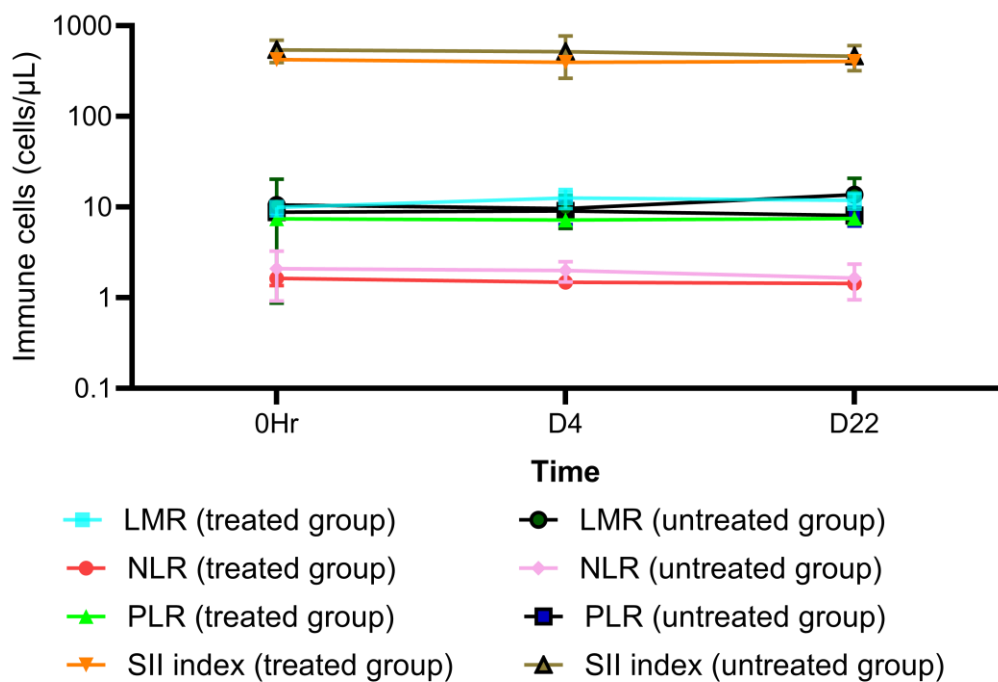

Figure 3. A comparison of different interleukin (IL) levels between the treated group and the untreated group for each day. NLRs: neutrophil-to-lymphocyte ratios; LMRs: lymphocyte-to-monocyte ratios; PLRs: platelet-to-lymphocyte ratios, SII: systemic-immune inflammatory index.
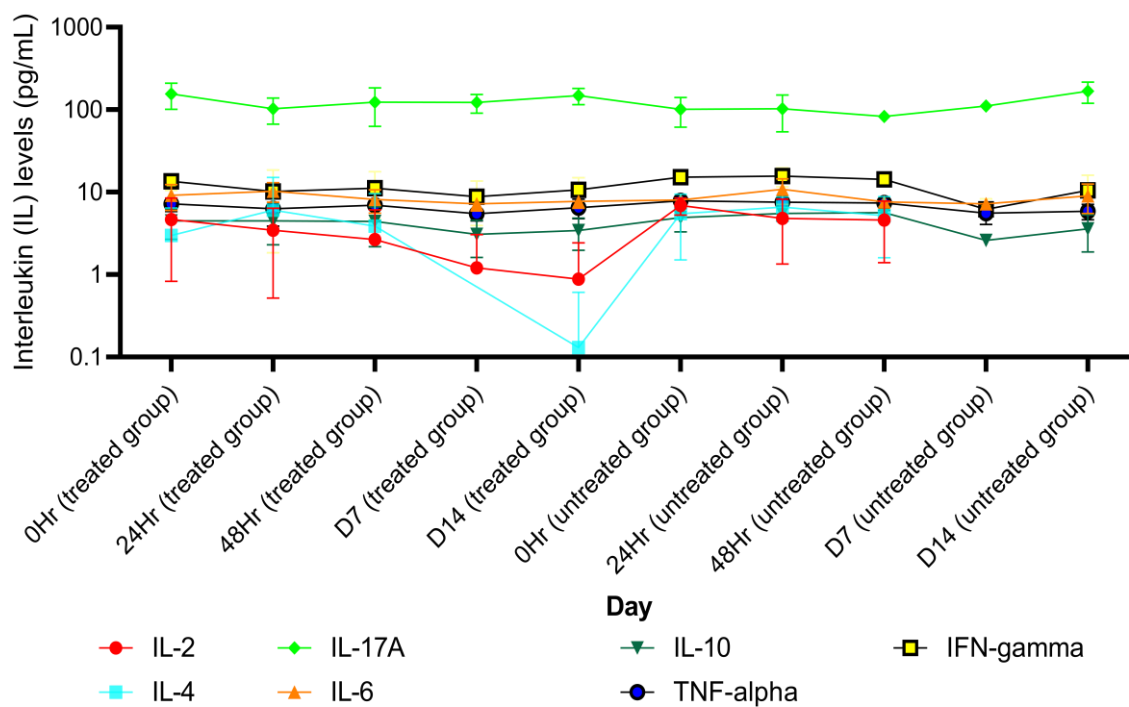
Figure 4. A comparison of different peripheral blood immune cells, peripheral blood index, and SII index between the treated group and the untreated group for each day. IL: interleukin; IFN-gamma: tumor necrosis factor gamma; TNF-alpha: tumor necrosis factor alpha.

2.3. Model Validation and Sensitivity Analysis

The overall AAFEs was 1.17. AAFEs for $AUC_{0\text{-}inf}$, C_{max}, CL/F, Vz/F, and $t_{1/2}$ for each group are summarized in Table S4. VPCs (predicted versus clinical values) are shown in Figures S1–S3. The sensitivity coefficients for P_{app}, $R_{b:p}$, solubility, pK_a, and f_u were +0.56, −0.90, +0.058, +0.14, and −0.18, respectively. A schematic workflow is shown in Figure 5.
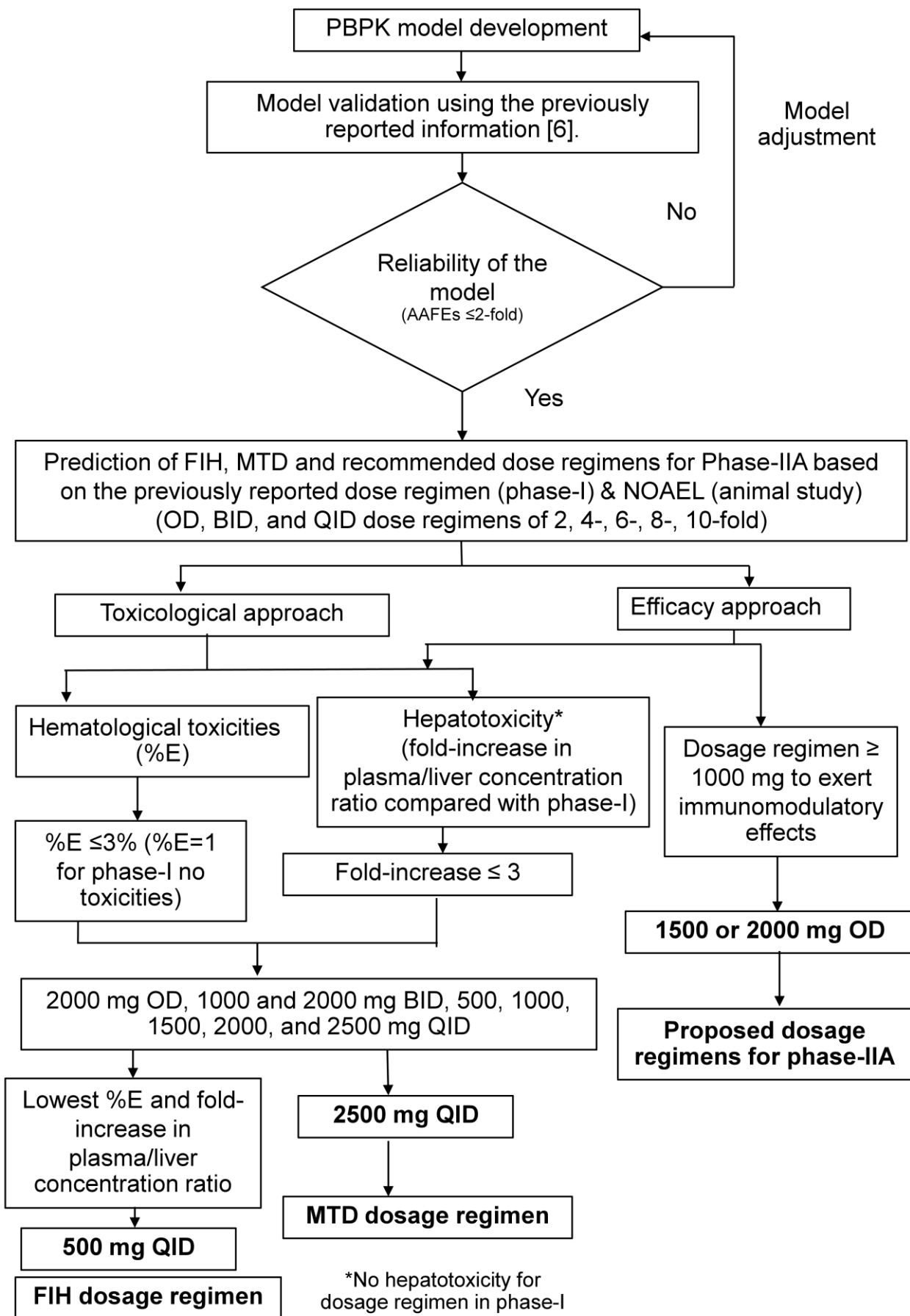
Figure 5. Schematic workflow criteria for dose selection. PBPK: physiologically based pharmacokinetic; BID: twice daily dose; FIH: first-in-human; OD: once-daily dose; MTD: maximal-tolerated

dose; NOAEL: non-observed adverse effect levels; QID: fourth times daily. This figure outlines the processes involved in developing a PBPK model and the guidelines for choosing dosage schedules based on the toxicities and immunomodulatory effects of AL, which encompass FIH, MTD, and suggested dosage plans for phase IIA.

2.4. Safety Assessment of the Simulated AL Regimens

2.4.1. Hematological Toxicities

The risks of hematological toxicity (%E) following an OD dose of 1000 mg AL administered for 21 days and 10 months were $1 \cdot 06 \pm 0 \cdot 31\%$ and $1 \cdot 08 \pm 0 \cdot 29\%$, respectively. When the dose was increased 2-fold (2000 mg), 4-fold (4000 mg), 6-fold (6000 mg), 8-fold (8000 mg), and 10-fold (10,000 mg), the risk increased to $2.24 \pm 0.70\%$, $5.26 \pm 1.38\%$, $7.30 \pm 1.73\%$, 8.76 ± 2.39, and $9.44 \pm 2.36\%$, respectively. The %E following the BID dose of 1000 mg AL (2000 mg total) administered for ten months was $1.13 \pm 0.32\%$. When each dose of the BID regimen was increased to 2000 mg (4000 mg total), 3000 mg (6000 mg total), 4000 mg (8000 mg total), and 5000 mg (10,000 mg total), the %E increased to $2.21 \pm 0.68\%$, $3.8 \pm 1.09\%$, $5.61 \pm 1.65\%$, and $6.89 \pm 1.5\%$, respectively. The %E following the QID dose of 500 mg AL (2000 mg total), 1000 mg AL (4000 mg total), 1500 mg AL (6000 mg total), 2000 mg AL (8000 mg total), and 2500 mg AL (10,000 mg total) administered for ten months were $0.30 \pm 0.11\%$, $1.29 \pm 0.53\%$, $1.95 \pm 0.54\%$, $2.45 \pm 0.62\%$, and $3.27 \pm 0.68\%$, respectively.

2.4.2. Hepatotoxicities

The $C_{max, u, liver}$ ratios of AL, when given an OD dose of 1000 mg for both 21 days and 10 months, increased 1.15-fold. When AL administration was extended to 10 months, increasing AL doses to 2000, 4000, 8000, and 10,000 mg resulted in 1.40-, 3.73-, 5.40-, 6.50-, and 7.07-fold increases in liver enzyme levels, respectively. For the 10-month BID regimens, AL at 1000, 2000, 3000, 4000, and 5000 mg resulted in 0.67-, 1.34-, 2.46-, 3.82-, and 4.74-fold increases in liver enzyme levels, respectively. For the 10-month QID regimens, AL at the doses of 500, 1000, 1500, 2000, and 2500 mg resulted in 0.17-, 0.71-, 1.07-, 1.40-, and 1.9-fold increases in liver enzyme levels, respectively.

3. Discussion

The PBPK model developed here is credible as the AAFEs were within 1.2-fold (≤2-fold), and none of the sensitivity coefficients were higher than 1.

3.1. FIH Dose Regimen

For the FIH dose regimens, the QID doses of 500 mg AL resulted in the lowest risks of hematological and liver toxicities compared with other regimens. Even with the higher total daily dose of 2000 mg (human equivalent dose or HED = 2400 mg) [6], which is about 2.5-fold lower than the observed non-observed adverse effect level (NOAEL) of 5000 mg/kg observed in animals [6], the risks of hematological and liver toxicities remained low. The FIH dose, determined based on the toxicological criteria, appears safe and is lower than that used in the previous phase 1 study. A result from the phase 1 clinical trial suggests that this estimation of FIH, based on the information obtained from a pilot study and PBPK modeling, would provide a safe starting dose regimen for a drug candidate and avoid using an unnecessarily large number of research participants.

3.2. The MTD Regimens

The %E following the OD dose of 1000 mg AL administered for 21 days was low (1%). This finding is consistent with the clinical data [6], supporting the validity of the Emax model for predicting the risk of hematological toxicity. The MTD regimen for AL was the QID dose of 2500 mg AL given for up to 10 months, with a %E of ≤5%, resulting in 2-fold increases in the upper limit normal (ULN) of AST, and ALT levels, indicating the high safety profiles of this drug even with the high dosage administration. This risk is relatively low, and the side effects associated with AL are uncommon. Notably, this dose level is only about 50% of the observed NOAEL in the animal study [5]. However, this dosage regimen might not be appropriate for clinical use due to the high bulk at 10,000 mg daily.

The risk of hematological toxicity following the OD regimen of 10,000 mg AL was lower than 10%. It did not impact hematological cells but was more potent than the BID regimen (also 10,000 mg total). Similarly, the risk of hepatotoxicity following the OD and BID regimens seemed to be increased, with AST and ALT levels increasing to 7-fold (grade-3) and 5-fold (grade-2) the ULN, respectively. Therefore, these two regimens are unsuitable for MTD dosage regimens due to the high risk of hepatotoxicity.

It has been reported that the conventional chemotherapy for iCCA (gemcitabine/cisplatin) is associated with grades 3–4 hematological toxicities, e.g., neutropenia (odds ratio (OR) = 2.80, $p < 0.001$), leukopenia (OR = 2.98, $p < 0.001$), and anemia (OR = 2·96, $p < 0.001$) [9]. A significant decrease in neutrophils was observed in 25% of the patients [10,11], of which 40% developed secondary infections [11]. In addition, gemcitabine/cisplatin was associated with liver toxicities [4,10,11], such as elevated levels of ALT (51.2%) and AST (53.5%) by >3-fold of ULN [4]. For second-line FOLFIRI-based chemotherapy (5-fluorouracil/irinotecan), 14.3% of the patients had increased ALT levels of grade 1 or 2 (>3-fold of ULN), and 85.7% had ascites [10].

3.3. Recommended AL Dose Regimens for Phase-2A Clinical Trial

A 1500 or 2000 mg AL QID dose is advised for phase-2A clinical trials in patients with advanced-stage CCA. The risks of hematological and liver toxicities following both regimens were lower than 3% and 1.5-fold (<3-fold of ULN). Notably, toxicities following most dose regimens of 1500 mg AL are unlikely to occur since the surrogate indicators for toxicities are similar to those described in the previous study (<2-fold of ULN) [5]. It is noted that a dose of AL of at least 1000 mg/day is required for immunomodulatory effects to be seen [5]. The OD (1500 or 2000 mg) regimens are promising for phase-2A trials since the risks of toxicities were lower than QID regimens with higher compliance. Therefore, the OD dose of 1000 and 2000 mg was used in phase 2A clinical trial. Preliminary results revealed that a once-daily OD dose of 2000 mg provided a significantly higher disease control rate (DCR), inhibition of increased tumor size, median overall survival (median OS), overall survival rate (OSR), progression-free survival (PFS), and progression-free survival rate (PFSR) in patients with unresectable or metastatic iCCA without toxicities compared with a once-daily OD dose of 1000 mg.

3.4. The Roles of Circulating Peripheral Cytokines and Peripheral Immune Cells in iCCA Therapy Based on Immunological Classification

The increase in peripheral immune cells has been reported to be directly related to promoting immune cell recruitment in the TME [12]. The present study evaluated the effects of peripheral blood cells and pro-inflammatory cytokines on AL activity. Modulation (suppression or stimulation) of circulating peripheral immune cells, peripheral blood cells, and circulating cytokines may be surrogates for these cells at the TME and tumor sites. Recent research revealed an increase in OS (overall survival) for CCA patients with substantial infiltration of B lymphocytes [13]. AL has also been reported to facilitate the

recruitment of immune cells to the TME by inhibiting the synthesis of matrix metalloproteinases (MMP-2 and MMP-9) [14], thus reducing fibrosis. AL also decreased the number of CD4+ cells. A high proportion of CD4+ circulating cells was associated with shorter recurrence-free survival (RFS) in CCA patients following surgery [15]. A decrease in LMR (≤4·17) was associated with favorable treatment outcomes in CCA [16]. AL raised LMR (Figure 3) but differed minimally from the baseline. Any impact of AL on LMR was unlikely. However, information on the CD4+/CD8+ ratio in CCA is limited, although an increase in the CD4+/CD8+ ratio has been associated with an improved prognosis in hepatocellular carcinoma following transarterial chemoembolization (TACE) [17]. Besides peripheral immune cells, AL significantly reduced the production of all pro-inflammatory cytokines. Decreases in IL-4, IL-6, and IL-17A levels were associated with substantial improvements in CCA burden, OS, disease progression, and metastasis [18–22]. Inhibition of IL-4 production is crucial for the development of M2 TAMs and MDSCs in the TME [23], as well as for the activation of mitogen-activated protein kinase (MAPK) [23]. A decrease in IL-4 receptor expression and increased tumor cell apoptosis was also observed [23]. IL-6 has been shown to inhibit CCA proliferation through the JAK-STAT3 (Janus kinase-signal transducer and activator of transcription-3) pathway and reduce the activity of M2 TAMs [24], thereby enhancing antitumor effects. It facilitates the recruitment of CD8+ and NK cells for IL-10 inhibition (CD94/NK group-2 member) [23]. IL-6 also suppresses the expression of lymphocyte activation gene-3 (LAG-3) and PD-1 (programmed cell death protein-1) on CD8+ cells in the TME [23], thus preventing T cell exhaustion. Suppression of IL-2 production improves the function of CD8+ and NK cells, increases the activity of regulatory T cells (Treg) at the IL-2 receptor, and suppresses CD8+ effector T cell function [25,26]. A decrease in TNF-α and IFN-γ production might impair the functions of both NK and CD8+ cells. In the present study, however, there was only a modest change in the levels of both these cytokines in response to AL, compared with the baseline. The suppression of IL-10 expression by AL led to increased production of IFN-γ and TNF-α and promoted the function of CD8+ effector T cells.

Advances in the knowledge of TME and molecular analysis in recent years have facilitated the search for new iCCA treatments. By enhancing the effects of immunosurveillance, ICIs become a new possible therapeutic approach for iCCA therapy. As CD8+ function boosters, anti-PD1 (e.g., pembrolizumab and nivolumab) and anti-PD-L1 (e.g., atezolizumab) are effective against a variety of solid tumors, except iCCA [3]. Despite the expression of PD-L1 on tumor-associated immune cells, the depletion of T cells induced by drugs is unlikely to be adequate for iCCA therapy. However, nivolumab with gemcitabine/cisplatin has been reported to improve OS [4]. Gemcitabine may diminish the number of circulating immunosuppressive cells (i.e., MDSCs) and induce the expression of MHC-I (major histocompatibility complex) in cancer cells (increasing antigenicity) [27], which supports the function of CD8+ cells. The absence of T cells in CCA tumors is attributed to the prevalence of immunological desert iCCA (I1: 48%) [2]. In contrast to other solid tumors, the treatment approach for iCCA involves transforming the tumor immunological type from cold to hot. The stromal cells and extracellular matrix (ECM) around the iCCA TME impede immune cell recruitment. Combining AL with gemcitabine/cisplatin, followed by an anti-PD1, is recommended for patients with advanced-stage iCCA. AL supports the recruitment of essential immune cells and facilitates dendritic cells (DC, MHC-I/II) to the tumor site by reducing fibrosis. On the other hand, gemcitabine boosts the function of MHC-I/II by increasing the immunogenicity of iCCA, and anti-PD1 reinvigorates CD8+ cell function. During the treatment of immunogenic iCCA (I2: 9%) [2], immune-stimulating cells must outweigh the activity of immunosuppressive cells. The key characteristic of therapy for immunogenic iCCA is promoting the activity of immunostimulating cells to exceed that of immunosuppressive cells. A combination of nivolumab

and AL is recommended. It has been reported that AL also supports the function of NK and CD8+ cytotoxic T cells. In addition, it inhibits the activity of Treg cells (through IL-2R inhibition) [25], which outweighs immuno-stimulating cell function. For myeloid iCCA (I3: 13%) [2], combination therapy of AL with any ICIs is recommended. Similarly, AL enhances the recruitment of antitumor immune cells, particularly CD8+ cells, to the tumor site. It also limits the recruitment of M2 TAMs by inhibiting the production of IL-4 and IL-10, thereby enhancing the functions of CD8+ and NK cells. ICIs also reverse the function of CD8+ cells in the TME. AL in combination with an anti-fibrotic agent, followed by gemcitabine/cisplatin, is suggested for mesenchymal iCCA (I4: 28%) [2] as it supports the reduction in tumor cell fibrosis through inhibition of MMP-2, and MMP-9 [14], thus augmenting the cytotoxic effects and facilitating the recruitment of CD4+, CD8+, and NK cells. For gemcitabine/cisplatin-resistant CCA, FOLFOX (folinic acid, 5-fluorouracil, and oxaliplatin), combined with ICIs, is recommended for increasing antigenicity [27].

The current study's limitations include a small sample size and the relatively low age of the virtual population (18–60 years in the placebo and AL-treated groups). In contrast, the average age of most patients with advanced-stage CCA is relatively older. The impact of the immunomodulatory effects of AL in patients with advanced-stage CCA may differ from healthy subjects. A phase-2A clinical trial with an adequate sample size is recommended to confirm the efficacy and safety of the proposed regimens. Since AL, specifically atractylodin, is an immunomodulator, the immune-modified response evaluation criteria for solid tumors (imRECIST) are suggested for evaluating tumor response endpoints due to the delayed impact of immunomodulators on tumor response.

4. Materials and Methods

4.1. Data Sources

The following data were obtained from a previous study in healthy Thai subjects: (i) plasma concentration–time profiles of atractylodin [6], the active component of AL, following a single dose of 1000 mg AL (group 1) and once-daily (OD) doses administered for 21 days (group 2), and (ii) parameters related to immunomodulatory activity, i.e., peripheral blood immune cells, and levels of pro-inflammatory cytokines following the OD of 1000 mg AL or placebo administered for 21 days (group 2) [5]. This study was retrospectively registered on 17 October 2020 [Thai Clinical Trials Registry (TCTR: www.clinicaltrials.in.th) (accessed on 7 July 2022) on Number TCTR20201020001]. The study was approved by the Ethics Committee of Thammasat University (No. TU-MED 2018-021, dated 23 May 2018) and Sakhon Na-Kon Hospital (No. 049/2020). The study was conducted following Good Clinical Practice (GCP) guidelines and the Declaration of Helsinki.

4.2. Pharmacokinetic Analysis

The pharmacokinetic parameters of atractylodin were estimated using non-compartmental analysis (MonolixSuite Software, version 2021R1, Antony France, Lixoft, SAS, 2021). The parameters included area under the plasma concentration–time curve (AUC_{0-inf}), maximum plasma concentration (C_{max}), terminal half-life ($T_{1/2}$), volume of distribution (V_z/F), and clearance (CL/F).

4.3. Statistical Analysis

Peripheral blood immune cell data collected included in the analysis were as follows: neutrophils, total lymphocytes, T cells, B cells, CD8+, CD4+, NK+ cells, CD4+/CD8+ ratio, lymphocyte-to-monocyte ratio (LMR), neutrophil-to-lymphocyte ratio (NLR), platelet-to-lymphocyte ratio (PLR), and systemic immune–inflammatory (SII) index. Circulating cytokines included IL-2, IL-4, IL-6, IL-10, TNF-α, and IFN-γ. The distribution of all variables

was assessed using the Shapiro–Wilk test. In addition, differences between the quantitative variables of the two groups were evaluated using the pair-*t* test (normally distributed variables) and the Wilcoxon match-pair signed ranked test (non-normally distributed variables). The statistical significance level was set at $\alpha = 0.05$. Single imputation was applied for missing data.

4.4. Model Construction

A whole-PBPK model of atractylodin was developed based on our in-house and previously published data [28] using Simbiology®, a product of MATLAB 2018b (version 5.8.2, MathWorks, Natick, MA, USA). Model assumptions were as follows: blood-flow restriction, rapid drug dissolution, absence of enterohepatic recirculation, and absence of stomach and large intestine absorption. The physicochemical and biochemical properties of atractylodin are summarized in Table S1.

4.5. Model Validation

The developed whole-PBPK model was validated against previously published clinical data. Absolute average-folding errors (AAFEs, Equation 1), and virtual predictive checks (VPCs) were used to determine model validity (accepted AAFEs ≤ 2-fold) [29].

$$AAFEs = \frac{\sum_{i=1,2,3,...n}^{n}\left|log\frac{prediction}{observation}\right|}{n} \tag{1}$$

Where *n* is the number of parameters. Prediction and observation are the predicted values and observed values, respectively.

4.6. Sensitivity Analysis

The sensitivity coefficient (Equation (2)) was computed to assess the uncertainty of the model parameters on atractylodin plasma-concentration profiles following an OD dose of 1000 mg AL for 21 days. A variation of 20% was applied to the fraction of unbound drug (f_u), apparent permeability (P_{app}), blood-to-plasma ratio ($R_{b:p}$), solubility, and negative log of the acid dissociation constant (pK_a).

$$Sensitivity\ coefficient = \frac{\%\nabla Y}{\%\nabla X} \tag{2}$$

where $\%\nabla Y$, and $\%\nabla X$ are the percent changes in atractylodin concentration–time profiles, and model parameters, respectively.

4.7. Prediction of MTD Dosage Regimens Based on Immunomodulatory Activities

Plasma concentration–time profiles of atractylodin were initially simulated using the OD dose of 1000 mg AL administered for 21 days, along with doses increased 2-, 4-, 6-, 8-, and 10-fold. The frequencies of administration were OD, twice daily (BID), and four times daily (QID). The maximum daily dose was 10,000 mg (10-fold) to minimize excessive dose administration and drug bulk.

4.8. Prediction of MTD Regimens Based on Toxicity Criteria

Emax model (Equation (3)) was applied to evaluate the hematological toxicity of atractylodin on the surrogate peripheral blood mononuclear cells (PBMCs) (5), following various AL regimens and was then compared with clinical data. The *%E* (reported as mean ± SD) was calculated to predict the maximal toxicity of atractylodin on PBMCs for each virtual population.

$$\%E = \left(\frac{E_{max}+C_p x f_u}{IC_{50,u}+C_p x f_u}\right) \tag{3}$$

where %*E* is the percentage of the toxicity of atractylodin on PBMCs. *Emax* is the maximum inhibitory effect (assumed to be 1 since the information is not available). *Cp* is atractylodin plasma concentration at time t. *IC$_{50,u}$* is the half-maximum inhibitory effect of unbound atractylodin concentration (*IC$_{50}$*=737 μmol/L) [6]. F$_u$ is the fraction of unbound atractylodin in plasma.

Besides the risk of hematological toxicity, hepatotoxicity of atractylodin was assessed based on the ratios between C$_{max}$ of unbound atractylodin in the liver (C$_{max, u, liver}$), following the OD administration. The increases in the levels of liver enzymes, i.e., aspartate aminotransferase (AST), alanine transaminase (ALT), and alkaline phosphatase (ALP) were used as surrogate markers for the risk of hepatotoxicity associated with each AL regimen. A positive linear relationship between daily dose regimen (up to 10,000 mg), and liver enzyme levels was also assumed. The C$_{max, u, liver}$ following the OD 1000 mg regimen was considered non-hepatotoxic (no elevation of liver enzymes in any subject) (6).

4.9. Virtual Population Simulation

%E, and the C$_{max, u, liver}$ following various dose regimens of AL were simulated (Monte Carlo) with 100 virtual populations (18–60 years old, healthy subjects, average weight of 60 kg, and in fasting state). Since the overall survival (OS) in advanced-stage CCA patients is 10 months [30], the risk of toxicity for this duration was predicted. For the purpose of predicting hematological and liver toxicity, AL treatment simulations were performed as 21-day courses.

5. Conclusions

The developed PBPK model accurately predicted the disposition of AL with AAFEs of 1·2-fold. Therefore, the suggested FIH and MTD regimens of AL are QID doses of 500 and 2500 mg, respectively. In addition, the recommended dosage regimens for phase 2A are OD doses of 1500 or 2000 mg. Notably, AL in conjunction with ICIs is recommended for each class of iCCA based on TME data to improve the clinical efficacy of AL.

6. Patents

Not applicable.

Abbreviations

AAFEs, absolute average-folding errors; AL, *Atractylodes lancea* Thunb (DC); ALP, alkaline phosphatase; ALT, alannine transminase; AST, aspartate aminotransferase; AUC, area under the plasma concentration–time curve; BID, twice-daily dose; CAF, cancer-associated fibroblast; C$_{max}$, maximum plasma concentration; C$_P$, plasma concentration at time t; DCR, disesae control rate; EMA, European Medicine Agency; E$_{max}$, maximum inhibitory effect; FIH, first-in-human; F$_u$, fraction of unbound drug; GCP, Good Clinical Practice; HED, human equivalent dose; IC$_{50,u}$, half-maximum inhibitory effect of unbound drug; iCCA, intrahepatic cholangiocarcinoma; IFN-γ, interfefron-gamma; IL, interleukins; imRECIST, immune-modified response evelution criteria for solid tumors; LAG-3, lymphocyte activation gene-3; MMP, matrix metalloproteinases; JAK-STAT3, Janus kinase-signal transducer and activator of transcription-3; NK, natural killer cells; NLR, neutrophil-to-lymphocyte ratios; MAPK, mitogen-activated protein kinase; MHC-I, major histocompatibility complex-I; MHC-II, major histocompatibility complex-II; MDSCs, myeloid-derived suppressive cells; MRSD, maximum recommended starting dose; MTD, maximum tolerated dose; NOAEL, non-observed adverse effect level, OD, once-daily; OR, odd ratio; OS, overall survival; OSR, overall survival rate; PBPK, physiologically based pharmacokinetic; P$_{app}$, apparent permeability; PBMCs, peripheral mononuclear cells; PD-1, programmed cell death protein 1; pK$_a$, negative log of the acid dissociation constant; PFR, progression-free survival; PFSR, progression-free survival rate; PLR,

platelet-to-lymphocyte ratios; QID, four time-daily dose; $R_{b:p}$, blood-to-plama ratios; SII index, systemic immune inflammatory index; TACE, transarterial chemoembolization; TAM, tumor-associated macrophage; TCM, traditional chinese medicine; TME, tumor microenvironment; TNF-α, tumor necrosis factor alpha; VPC, virtual predictive check; ULN, upper limit normal; US FDA, U.S. Food and Drug Administration.

Supplementary Materials: The following supporting information can be downloaded at www.mdpi.com/xxx/s1, Figure S1: A comparison of atractylodin plasma concentration–time profiles following a single dose of 1000 mg of *Atractylodes Lancea* (Thunb) DC on day 1 between predicted values and clinical data. Figure S2: A comparison of atractylodin plasma concentration–time profiles following multiple doses of 1000 mg of *Atractylodes Lancea* (Thunb) DC on day 1 between predicted values and clinical data. Figure S3: A comparison of atractylodin plasma concentration–time profiles following multiple doses of 1000 mg of *Atractylodes Lancea* (Thunb) DC on day 21 between predicted values and clinical data. Table S1: Model parameters. Table S2: A statistical analysis of circulating cytokines following successive doses of 1000 mg of AL administered for 21 days. Table S3: A statistical analysis of peripheral blood immune cells, SII index, NLR, LMR, PLR, and SII index following daily doses of 1000 mg of AL administered for 21 days. Table S4: Model validation.

Author Contributions: T.S.: conceptualization: lead; data curation: lead; formal analysis: lead; investigation: lead; methodology: lead; validation: lead; software: lead; visualization: lead; writing—original draft: lead. J.K.: conceptualization: support; data curation: support; formal analysis: support; investigation: support; methodology: support; project administration: lead; resources: support; writing—review and editing: lead. K.N.-b.: conceptualization: lead; data curation: lead; formal analysis: lead; funding acquisition: lead; investigation: lead; methodology: lead; project administration: lead; resources: lead; software: lead; visualization: lead; writing—review and editing: lead. All authors have read and agreed to the published version of the manuscript.

Institutional Review Board Statement: The study was conducted in accordance with the Declaration of Helsinki, and approved by the Institutional Review Board (or Ethics Committee) of Thammasat University (No. TU-MED 2018-021, dated 23 May 2018) and Sakon Nakorn Hospital (protocol code 049/2020 and date of approval: 02 February 2021).

Informed Consent Statement: Informed consent was obtained from all subjects involved in the study.

Data Availability Statement: The original contributions presented in this study are included in the article/supplementary material. Further inquiries can be directed to the corresponding author(s).

Conflicts of Interest: The authors declare no conflicts of interest. The funders had no role in the study's design, in the collection, analyses, or interpretation of data, in the writing of the manuscript, or in the decision to publish the results.

References

1. Loeuillard, E.; Conboy, C.B.; Gores, G.J.; Rizvi, S. Immunobiology of cholangiocarcinoma. *JHEP Rep.* **2019**, *1*, 297–311.

2. Job, S.; Rapoud, D.; Dos Santos, A.; Gonzalez, P.; Desterke, C.; Pascal, G.; Elarouci, N.; Ayadi, M.; Adam, R.; Azoulay, D.; et al. Identification of four immune subtypes characterized by distinct composition and functions of tumor microenvironment in intrahepatic cholangiocarcinoma. *Hepatology* **2021**, *72*, 965–981.

3. Gutiérrez-Larrañaga, M.; González-López, E.; Roa-Bautista, A.; Rodrigues, P.M.; Díaz-González, Á.; Banales, J.M.; López-Hoyos, M.; Santos-Laso, A.; Crespo, J. Immune checkpoint inhibitors: The emerging cornerstone in cholangiocarcinoma therapy? *Liver Cancer* **2021**, *10*, 545–560.

4. Ueno, M.; Ikeda, M.; Morizane, C.; Kobayashi, S.; Ohno, I.; Kondo, S.; Okano, N.; Kimura, K.; Asada, S.; Namba, Y.; et al. Nivolumab alone or in combination with cisplatin plus gemcitabine in Japanese patients with unresectable or recurrent biliary tract cancer: A non-randomised, multicentre, open-label, phase 1 study. *Lancet. Gastroenterol. Hepatol.* **2019**, *4*, 611–621.

5. Kulma, I.; Panrit, L.; Plengsuriyakarn, T.; Chaijaroenkul, W.; Warathumpitak, S.; Na-Bangchang, K. A randomized placebo-controlled phase I clinical trial to evaluate the immunomodulatory activities of Atractylodes Lancea (Thunb) DC. in healthy Thai subjects. *BMC Complement. Altern. Med.* **2021**, *21*, 61.

6. Na-Bangchang, K.; Kulma, I.; Plengsuriyakarn, T.; Tharavanij, T.; Kotawng, K.; Chemung, A.; Muhamad, N.; Karbwang, J.. Phase I clinical trial to evaluate the safety and pharmacokinetics of capsule formulation of the standardized extract of Atractylodes Lancea. *J. Trad. Complement. Med.* **2021**, *11*, 343–355.

7. Shebley, M.; Sandhu, P.; Riedmaier, A.E.; Jamei, M.; Narayanan, R.; Patel, A.; Peters, S.A.; Reddy, V.P.; Zheng, M.; de Zwart, L.; et al. Physiologically based pharmacokinetic model qualification and reporting procedures for regulatory submissions: A consortium perspective. *Clin. Pharmacol. Ther.* **2018**, *104*, 88–110.

8. Zhao, P. Report from the EMA workshop on qualification and reporting of physiologically based pharmacokinetic (PBPK) modeling and simulation. *CPT Pharmacomet. Syst. Pharmacol.* **2017**, *6*, 71–72.

9. Liu, H.; Zhang, Q.D.; Li, Z.H.; Zhang, Q.Q.; Lu, L.G. Efficacy and safety of gemcitabine-based chemotherapies in biliary tract cancer: A meta-analysis. *World J. Gastroenterol.* **2014**, *20*, 18001–18012.

10. Möhring, C.; Feder, J.; Mohr, R.U.; Sadeghlar, F.; Bartels, A.; Mahn, R.; Zhou, T.; Marinova, M.; Feldmann, G.; Brossart, P.; et al. First line and second line chemotherapy in advanced cholangiocarcinoma and impact of dose reduction of chemotherapy: A retrospective analysis. *Front. Oncol.* **2021**, *11*, 717397.

11. Valle, J.; Wasan, H.; Palmer, D.H.; Cunningham, D.; Anthoney, A.; Maraveyas, A.; Madhusudan, S.; Iveson, T.; Hughes, S.; Pereira, S.P.; et al. Cisplatin plus gemcitabine versus gemcitabine for biliary tract cancer. *N. Engl. J. Med.* **2020**, *362*, 1273–1281.

12. Griffiths, J.I.; Wallet, P.; Pflieger, L.T.; Stenehjem, D.; Liu, X.; Cosgrove, P.A.; Leggett, N.A.; McQuerry, J.A.; Shrestha, G.; Rossetti, M.; et al. Circulating immune cell phenotype dynamics reflect the strength of tumor-immune cell interactions in patients during chemotherapy. *Proc. Nat. Acad. Sci. USA* **2020**, *117*, 16072–16082.

13. Goeppert, B.; Frauenschuh, L.; Zucknick, M.; Stenzinger, A.; Andrulis, M.; Klauschen, F.; Joehrens, K.; Warth, A.; Renner, M.; Mehrabi, A.; et al. Prognostic impact of tumor-infiltrating immune cells on biliary tract cancer. *Br. J. Cancer* **2013**, *109*, 2665–2674.

14. Jun, X.; Fu, P.; Lei, Y.; Cheng, P. Pharmacological effects of medicinal components of Atractylodes Lancea (Thunb) DC. *Chin. Med.* **2018**, *13*, 59.

15. Kida, A.; Mizukoshi, E.; Kido, H.; Toyama, T.; Terashima, T.; Arai, K.; Yamashita, T.; Fushimi, K.; Yamashita, T.; Sakai, Y.; et al. The characteristics of the immune cell profiles in peripheral blood in cholangiocarcinoma patients. *Hepatol. Int.* **2021**, *15*, 695–706.

16. Jin, B.; Hu, W.; Su, S.; Xu, H.; Lu, X.; Sang, X.; Yang, H.; Mao, Y.; Du, S. The prognostic value of systemic inflammation response index in cholangiocarcinoma patients. *Cancer Mag. Res.* **2021**, *13*, 6263–6277.

17. Ren, Z.; Yue, Y.; Zhang, Y.; Dong, J.; Liu, Y.; Yang, X.; Lin, X.; Zhao, X.; Wei, Z.; Zheng, Y.; et al. Changes in the peripheral blood Treg cell proportion in hepatocellular carcinoma patients after transarterial chemoembolization with microparticles. *Front. Immunol.* **2021**, *12*, 624789.

18. Cheon, Y.K.; Cho, Y.D.; Moon, J.H.; Jang, J.Y.; Kim, Y.S.; Kim, Y.S.; Lee, M.S.; Lee, J.S.; Shim, C.S. Diagnostic utility of interleukin-6 (IL-6) for primary bile drug cancer and changes in serum IL-6 levels following photodynamic therapy. *Am. J. Gastroenterol.* **2007**, *102*, 2164–2170.

19. Vainer, N.; Dehlendorff, C.; Johansen, J.S. Systematic literature review of IL-6 as a biomarker or treatment target in patients with gastric, bile duct, pancreatic, and colorectal cancer. *Oncotarget* **2018**, *9*, 29820–29841.

20. Wang, S.; Li, Z.; Hu, G. Prognostic role of intratumoral IL-17A expression by immunohistochemistry in solid tumors: A meta-analysis. *Oncotarget* **2017**, *8*, 66382–66391.

21. Yang, B.; Kang, H.; Fung, A.; Zhao, H.; Wang, T.; Ma, D. The role of interleukin 17 in tumour proliferation, angiogenesis, and metastasis. *Mediat. Inflamm.* **2014**, *2014*, 623759.

22. Zhou, M.; Wang, C.; Lu, S.; Xu, Y.; Li, Z.; Jiang, H.; Ma, Y. Tumor-associated macrophages in cholangiocarcinoma: Complex interplay and potential therapeutic target. *EBioMedicine* **2021**, *67*, 103375.

23. Mirlerkar, B. Tumor promoting roles of IL-10, TGF-β, IL-4, and IL-35: Its implications in cancer immunotherapy. *Sage Open Med.* **2022**, *10*, 20503121211069012.

24. Tsukamoto, H.; Fujieda, K.; Senju, S.; Ikeda, T.; Oshiumi, H.; Nishimaru, Y. Immune-suppressive effects of interleukin-6 on T-cell-mediated anti-tumor immunity. *Cancer Sci.* **2018**, *109*, 523–530.

25. Chinen, T.; Kannan, A.K.; Levine, A.G.; Fan, X.; Klein, U.; Zheng, Y.; Gasteiger, G.; Feng, Y.; Fontenot, J.D.; Rudensky, A.Y. An essential role of IL-2 receptor in Treg cell function. *Nat. Immunol.* **2016**, *17*, 1322–1333.

26. Ye, C.; Brand, D.; Zheng, S.G. Targeting IL-2: An unexpected effect in treating immunological diseases. *Signal Transduct. Target. Ther.* **2018**, *3*, 2.

27. Galluzzi, L.; Buque, A.; Kepp, O.; Zitvogel, L.; Kroemer, G. Immunological effects of conventional chemotherapy and targeted anticancer agents. *Cancer Cell* **2015**, *28*, 690–714.

28. Saeheng, T.; Na-Bangchang, K.; Siccardi, M.; Rajoli, R.K.R.; Karbwang, J. Physiologically-based pharmacokinetic modeling for optimal dosage prediction of quinine co-administered with ritonavir-boosted lopinavir. *Clin. Pharmacol. Ther.* **2020**, *107*, 1209–1220.

29. Saeheng, T.; Na-Bangchang, K.; Karbwang, J. Utility of physiologically based pharmacokinetic (PBPK) modeling in oncology drug development and its accuracy: A systematic review. *Eur. J. Clin. Pharm.* **2018**, *74*, 1365–1376.

30. Butthongkomvong, K.; Sirachainan, E.; Jhankumpha, S.; Kumdang, S.; Sukhontharot, O. Treatment outcome of palliative chemotherapy in inoperable cholangiocarcinoma in Thailand. *Asian Pac. J. Cancer Prev.* **2013**, *14*, 3565–3568.